IEEE Access
Multidisciplinary | Rapid Review | Open Access Journal

Received December 1, 2018, accepted December 10, 2018, date of publication December 21, 2018,
date of current version January 11, 2019.

Digital Object Identifier 10.1109/ACCESS.2018.2889222

A Horst-Type Power Divider With Wide Frequency Tuning Range Using Varactors

ANQI CHEN, YUAN ZHUANG, YI HUANG, (Senior Member, IEEE), AND JIAFENG ZHOU
Electrical Engineering and Electronics Department, University of Liverpool, Liverpool L69 3GJ, U.K.
Corresponding author: Jiafeng Zhou (zhouj@liverpool.ac.uk)

ABSTRACT This paper presents a novel power divider with a wide frequency tuning range. In our previous work, a pair of capacitors were connected in parallel with the front transmission lines of a Trantanella-type power divider introducing an additional reflection minimum, together with the original reflection zero to broaden the bandwidth. In this design, the latter transmission lines are removed. The added capacitors generate a reflection minimum, which can be easily controlled by varactors. Thus, the frequency band of the power divider can be flexibly tuned by altering the varactors. Design parameters are carefully chosen to eliminate the effect of the original reflection zero. By doing so, the power divider will have a tunable center frequency instead of a tunable bandwidth. Theoretical formulas for the characteristic impedances and electrical lengths of the transmission lines of the power divider are derived and analyzed. A power divider has been designed and fabricated to demonstrate the validity of the proposed design. The measured results indicate that the power divider can achieve a frequency tuning range of 0.9–4.2 GHz ($f_H/f_L = 4.67$:1), with in-band input and output return losses, both better than 22 dB, and an insertion loss of 3.2–4 dB. The measured in-band isolation is better than 15 dB. The power divider has a simple layout and a compact size of 0.2 $\lambda_g \times 0.16\ \lambda_g$, which demonstrates the excellent potential of the proposed power divider for modern communication systems.

INDEX TERMS Horst-type power divider, power dividers, tunable bandwidth, varactors.

I. INTRODUCTION

Nowadays modern communication systems usually need to support multi-communication standards, which require the components to have multiple operational bands. Power dividers are essential components in communication systems for power splitting and combining. The features of a power divider in terms of the operational frequency band, input/output return loss, and isolation between the output ports will significantly affect the overall performance of the communication system. Although many designs [1]–[3] of multi-band power dividers have been reported, their circuit size is usually bulky. Many modern wireless communication systems prefer tunable RF components instead of multiplexing into separated frequency bands due to the size and cost reduction. As the demand for spectrally cognitive microwave system is rising, more and more researches are focusing on frequency agile devices, such as reconfigurable couplers [4], resonators and filters [5]–[9]. With the rapidly increasing demands on multi-band feature of the power dividers, there is growing attention paid to power dividers with a compact size and wide tunable frequency ranges. Filtering tunable power dividers [10]–[12] have been investigated. In these designs, a filter and a power divider are cascaded to achieve a filtering response. The filter replaces the quarter-wavelength transmission lines in Wilkinson power dividers. The aim of such designs is to provide a filtering response to the power dividers. However, there are drawbacks. The insertion loss is relatively high (1.8-2.4 dB) due to the limited unloaded quality factor of microstrip resonators. Moreover, the port matching and isolation conditions are usually not satisfactory. To maintain the performance in the entire tunable frequency band, [13], [14] introduced coupled-line tunable Wilkinson power dividers which have excellent input and output impedance matching ($|S_{11}|, |S_{22}| < -17$ dB) and isolation ($|S_{23}| < -25$ dB). The aforementioned power dividers are good to be used in many filtering power divider applications. However, the limitation of the 20 dB tuning range (normally less than 2:1) is still a challenge. Modern transceivers like software defined radios require a wide range of radio spectrum. The designs in [15] and [16] have a tunable frequency range of 2.9:1 by employing short-electrical transmission lines along with a shunt varactor to the

Wilkinson-type power divider, but no analytical solutions to describe the relationship of capacitance and the corresponding frequency were provided. This paper proposes a novel power divider which has a wider tunable frequency band with a compact footprint. In our previous work [17], a pair of varactors were introduced in parallel with the front transmission lines. The predominant difference is that the design in [17] has one extra pair of transmission lines that connect the outputs with the isolation networks so that the frequency bandwidth of the divider can be tuned by the varactors. While the proposed divider in this work utilizes a Horst Divider structure [18], [19]. In this design, the extra transmission lines were removed to eliminate the original reflection zero and maintain the additional reflection minimum which is introduced by the added varactors. The reflection minimum is very sensitive to the capacitance change. As a result, the proposed design can achieve a very wide center frequency tuning range.

The center frequency of the operational band can be defined as the frequency of the corresponding reflection minimum. The center frequency moves along a locus. In other words, the center frequency can be flexibly controlled by the varactors. The example shown in this paper has achieved a frequency tuning range of 0.9- 4.2 GHz by properly tuning the varactors. Excellent output return loss and isolation response are retained over the whole tunable band. Moreover, good physical isolation between two output ports can be realized by using a Horst structure which is a pair of short-length-transmission lines connected between the front transmission lines and to the isolation circuit The good physical isolation not only separates two output ports but also suppresses the undesirable coupling between them. The design equations and analysis of the proposed structure are presented in Section II. In Section III, a prototype of the proposed power divider is fabricated and measured to validate the proposed theory. In the end, conclusions will be drawn in Section IV.

II. ANALYTICAL DESIGN EQUATIONS FOR THE PROPOSED POWER DIVIDER

The proposed reconfigurable power divider is presented in Fig. 1. A pair of varactors are added in parallel to the main transmission lines to realize tunability. As Fig. 1 shows, Z_0 represents the port impedance. Z_1 and Z_2 are the characteristic impedances of the front transmission lines and the transmission lines in the isolation circuit, respectively.

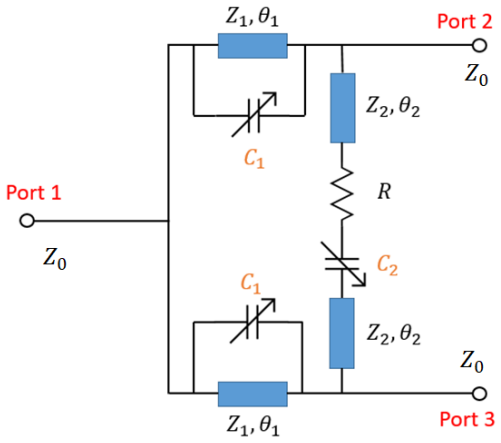

FIGURE 1. Structure of the proposed power divider.

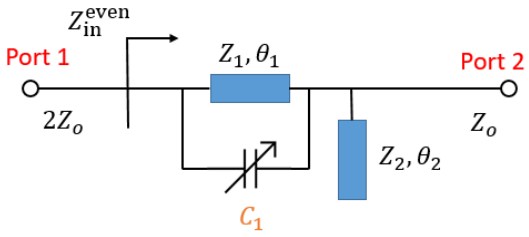

FIGURE 2. The equivalent circuit of the proposed structure for even-mode analysis.

C_1 represents the capacitance of the added varactors on the front transmission lines, C_2 is the capacitance of the varactor on the isolation circuit connected in series with a resistor. The electrical lengths of the transmission lines are defined as θ_1 and θ_2 at frequency f in the same way as θ_0 at the center frequency f_0. The relationship among the characteristic impedances, electrical lengths of the transmission lines and the varactors can be derived by an even-mode analysis method To design the isolation circuit, the odd-mode analysis method can be applied to calculate the lumped resistor R and varactor C_2.

A. EVEN-MODE ANALYSIS

The even-mode equivalent circuit of the proposed power divider is depicted in Fig. 2. The normalized ABCD matrix of the structure is in (1), as shown at the bottom of this page, where the frequency $\overline{f}$ is normalized to 1 GHz. The port impedance Z_0 is normalized to 1, and Z_1 and Z_2 are

$$\begin{bmatrix} \overline{A} & \overline{B} \\ \overline{C} & \overline{D} \end{bmatrix} = \begin{bmatrix} \dfrac{\overline{Y} - \frac{1}{\overline{Z_1}\tan(\theta_1\overline{f})}}{\overline{Y} - \frac{1}{\overline{Z_1}\sin(\theta_1\overline{f})}} & \dfrac{1}{j\left(\overline{Y} - \frac{1}{\overline{Z_1}\sin(\theta_1\overline{f})}\right)} \\ \dfrac{\left(\overline{Y} - \frac{1}{\overline{Z_1}\sin(\theta_1\overline{f})}\right)^2 - \left(\overline{Y} - \frac{1}{\overline{Z_1}\tan(\theta_1\overline{f})}\right)^2}{j\left(\overline{Y} - \frac{1}{\overline{Z_1}\sin(\theta_1\overline{f})}\right)} & \dfrac{\overline{Y} - \frac{1}{\overline{Z_1}\tan(\theta_1\overline{f})}}{\overline{Y} - \frac{1}{\overline{Z_1}\sin(\theta_1\overline{f})}} \end{bmatrix} \cdot \begin{bmatrix} 1 & 0 \\ j\dfrac{\tan(\theta_2\overline{f})}{\overline{Z_2}} & 1 \end{bmatrix}$$
$$\overline{Y} = 2\pi\overline{f} \cdot \overline{C_1} \tag{1}$$

normalized to Z_0, respectively. The normalized $\overline{C_1}$ equals to $C_1 \cdot Z_0$. The normalized input impedance of the circuit can be calculated by using the ABCD matrix as:

$$\overline{Z_{in}^{\text{even}}} = \frac{\overline{\text{A}} \cdot 1 + \overline{B}}{\overline{C} \cdot 1 + \overline{D}} \tag{2}$$

The magnitude of the return loss can be expressed as:

$$|S_{11}| = \left|\frac{\overline{\text{A}} + \overline{B}/1 - \overline{C} \cdot 1 - 2 \cdot \overline{D}}{\overline{\text{A}} + \overline{B}/1 + \overline{C} \cdot 1 + 2 \cdot \overline{D}}\right| = \sqrt{\frac{c^2 + d^2}{a^2 + b^2}}$$

$$\begin{cases} a = \left(\left(1 - 2\overline{PY}\right)\overline{Z_1}^2 + 2\right)\sin(\theta_1\bar{f}) \\ \quad + \overline{Z_1}\left(\left(4\overline{Y} + 2\overline{P}\right)\cos(\theta_1\bar{f}) + 4\overline{Y}\right) \\ b = \left(3\overline{Y} + \overline{P}\right)\overline{Z_1}^2\sin(\theta_1\bar{f}) - 3\cos(\theta_1\bar{f})\overline{Z_1}^2 \\ c = \left(\left(2\overline{PY} + 1\right)\overline{Z_1}^2 - 2\right)\sin(\theta_1\bar{f}) \\ \quad + \overline{Z_1}\left(4\overline{Y} - \left(4\overline{Y} + 2\overline{P}\right)\cos(\theta_1\bar{f})\right) \\ d = \left(\overline{P} - \overline{Y}\right)\overline{Z_1}^2\sin(\theta_1\bar{f}) + \overline{Z_1}\cos(\theta_1\bar{f}) \end{cases}$$

$$\overline{P} = \frac{\tan(\theta_2\bar{f})}{\overline{Z_2}} \tag{3}$$

The input port in Fig. 2 will be perfectly matched by solving:

$$\begin{cases} \text{Re}\left(\overline{Z_{in}^{\text{even}}}\right) = 2 \\ \text{Im}\left(\overline{Z_{in}^{even}}\right) = 0 \end{cases} \tag{4}$$

Hence, the characteristic impedance of the front transmission lines can be obtained by:

$$\overline{Z_1} = \frac{\left(2\overline{P} + \sqrt{8\overline{P}^2 + 2}\right)\sin(\theta_1\overline{f_Z})}{\left(\cos(\theta_1\overline{f_Z}) + 1\right) \cdot \left(2\overline{P}^2 + 1\right)}$$

$$\overline{P} = \frac{\tan(\theta_2\overline{f_Z})}{\overline{Z_2}} \tag{5}$$

Eq (5) suggests that with given θ_1, θ_2, $\overline{Z_1}$ and $\overline{Z_2}$, there exists a reflection zero at $\overline{f_z}$, where $|S_{11}|$ equals to 0. When $\overline{C_1}$ changes, (4) are no longer satisfied which means $|S_{11}|$ is not zero but is still close to zero. Thus, the reflection zero becomes a reflection minimum at frequency $\overline{f_m}$ that is close to $\overline{f_z}$. If θ_1, θ_2, $\overline{Z_1}$ and $\overline{Z_2}$ are properly chosen, $\overline{f_m}$ can be tuned by continuously changing $\overline{C_1}$, and the tuning range of $\overline{f_m}$ with $|S_{11}|$ in dB better than -20 dB represents the frequency tuning range of the circuit.

Let θ_1 and θ_2 be independent variables and are varying between 0° to 90°. Since θ_1 is the electrical length of the main transmission line, it can be assigned to determine the proper tuning band. While θ_2 should be chosen from small values such as $0° \leq \theta_2 \leq 20°$ to simplify the layout for practical applications. Moreover, it is necessary to bend the front transmission lines for placing the varactors in parallel with them, and to achieve a compact size of the topology. Hence, the ratio of length and width for the front transmission lines need to be sufficiently large for bending. Specifically, a larger θ_1 indicates longer transmission lines while lager $\overline{Z_1}$ implies narrower width of the transmission lines. Therefore, $\theta_1$and $\overline{Z_1}$ should be chosen appropriately for fabrication purposes.

B. FREQUENCY TUNING RANGE WITH $\overline{Z_1}$ AND $\overline{Z_2}$

This section discusses how to enhance the frequency tuning range by choosing appropriate values of $\overline{Z_1}$ and $\overline{Z_2}$. Using $\theta_1 = 30°$, $\theta_2 = 18°$ and $\overline{Z_2} = 2.5$ as an example, Fig. 3 depicts several calculated curves base on (5) which represent the relationship among $\overline{Z_1}$, $\overline{Z_2}$ and the normalized zero-reflection frequencies. If $\overline{Z_1}$ and $\overline{Z_2}$ has only one intersection, then we have only one zero-reflection frequency and in this case $\overline{Z_1} = \overline{Z}_{\text{match}}$. The intersection points of $\overline{Z_1} = 0.4$ and $\overline{Z_2} = 2.5$ have two corresponding frequencies $\overline{f_{m1}} = 1.4$ and $\overline{f_{m2}} = 4.5$ which are the normalized zero-reflection frequencies. Having two reflection zeros will result in different frequency tuning range comparing to that with only one reflection zero. As described in subsection *A*, continuously changing the value of $\overline{C_1}$ will result in a controllable variation of reflection minimum frequency $\overline{f_m}$. Thus, continuously tuning $\overline{C_1}$ can produce consecutive frequency minima which form an envelope curve of $|S_{11}|$ in dB. The frequency tuning range can be determined by the envelope curve as it records the movement of the $|S_{11}|$ trough over the whole operating band. Fig. 4(a)-(d) depicts six sampled $|S_{11}|$ curves with different values of $\overline{C_1}$. The dashed line is the envelope curve drawn to illustrate the troughs of $|S_{11}|$ curves over the whole frequency band. Let $\overline{Z_1} = \alpha \cdot \overline{Z}_{\text{match}}$, where α is a rational factor. Fig. 4(a) represents the case when $\overline{Z_1} = \overline{Z}_{\text{match}}$, where $\alpha = 1$. There is only one zero-reflection point over the tuning range. In this case, the center frequency tuning range is relatively narrow. If α increases, for instance, $\alpha = 1.15$, the reflection zero disappears, and the minimum of the $|S_{11}|$ envelope would be worse than infinity and the tuning range would shrink as shown in Fig. 4(b). Conversely, there will be two reflection zeros on the $|S_{11}|$ envelope curve if α decreases from 1 (eg. $\alpha = 0.85, 0.6$) as shown in Fig. 4(c) and (d). In this case, the frequency tuning

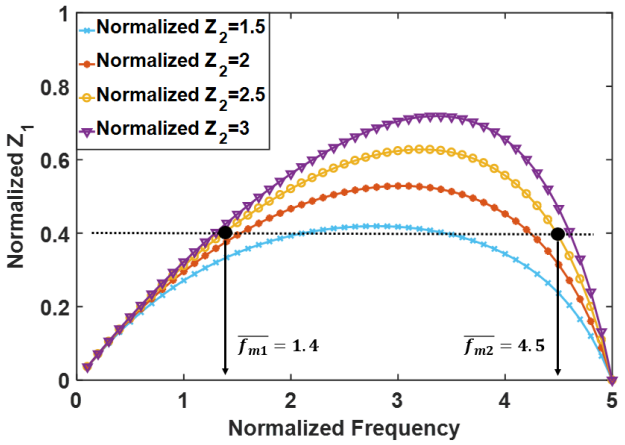

FIGURE 3. Theoretical reflection zero frequency curve with changing $\overline{Z_1}$ and $\overline{Z_2}$.

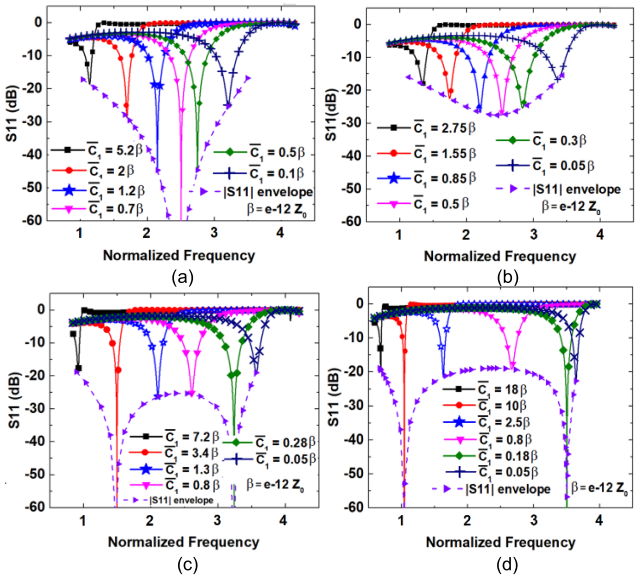

FIGURE 4. Theoretical S_{11} envelope curves as a function of $\overline{C_1}$ for different impedance of front transmission lines for (a) α=1, (b) α=1.15, (c) α=0.85 and (d) α=0.6.

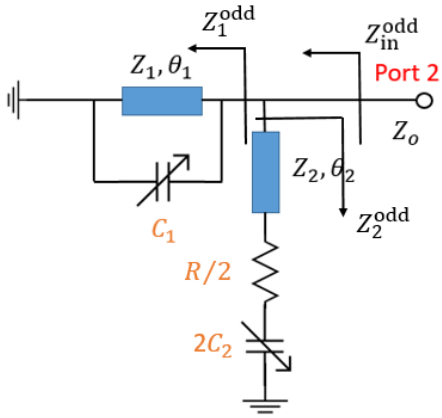

FIGURE 5. Odd-mode equivalent circuit for the proposed tunable power divider.

range can be extended by controlling the distance between the two reflection zeros. A larger distance between the minima leads to a wider tuning range. However, the performance of S_{11} between the two zeroes will be sacrificed.

C. ODD-MODE ANALYSIS

The odd-mode equivalent circuit of the power divider is shown in Fig. 5. To achieve perfect impedance matching at the output the following conditions should be satisfied:

$$\begin{cases} \mathrm{Re}\left(\overline{Z_{in}^{odd}}\right) = 1 \\ \mathrm{Im}\left(\overline{Z_{in}^{odd}}\right) = 0 \end{cases} \tag{6}$$

By substituting design parameters to (6), the total impedance of the isolation circuit can be calculated as in (7), as shown at the bottom of this page.

Thus, the capacitance $\overline{C_2}$ and resistance $\overline{R}$ in the isolation circuit can be obtained by solving:

$$\begin{cases} \mathrm{Re}\left(\overline{Z_{\mathrm{ISO}}}\right) = \overline{R}/2 \\ \mathrm{Im}\left(\overline{Z_{ISO}}\right) = 1/2\omega\overline{C_2} \end{cases} \tag{8}$$

Since $\overline{Z_1}$, $\overline{Z_2}$, θ_1 and θ_2 have been chosen from the even-mode analysis, a proper range of $\overline{C_2}$ can be determined by substituting different values of capacitance $\overline{C_1}$ to (8).

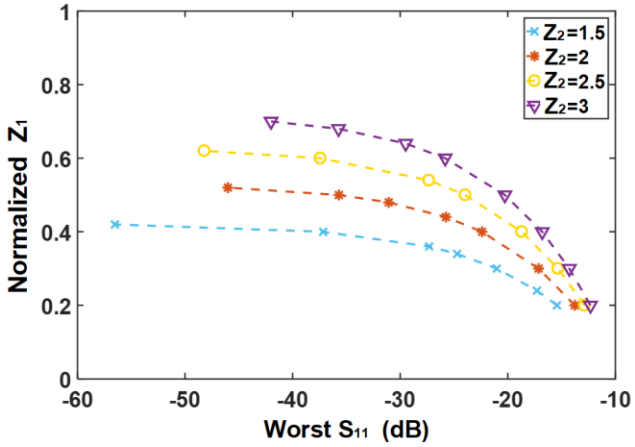

FIGURE 6. The relationship between the worst in-band $|S_{11}|$ and changing $\overline{Z_1}$.

D. TUNING RANGE OF THE POWER DIVIDER

Since each $|S_{11}|$ curve has only one trough which is the reflection minimum, the expression of the $|S_{11}|$ envelope curve can be calculated based on the derivation of $|S_{11}|$ regarding frequency. The synthesis method is discussed in the Appendix. In this case, the relationship between $\overline{C_1}$ and $\overline{f_m}$ can be obtained by (9), as shown at the top of the next page, and the $|S_{11}|$ envelope curve expression can be given as (11). One crucial parameter to be considered here is the worst in-band $|S_{11}|$. Although a larger difference between the two reflection zeros indicates a larger tuning range, the crest of the S_{11} envelope should be better than the specified value. For example, if $|S_{11}|$ should be better than -20 dB, α should be greater than 0.6 because $|S_{11}|$ exceeds -20 dB at the center frequency as shown in Fig. 4(d), which would not meet the design specification. Mathematically, the worst in-band S_{11} can be calculated by taking the derivative of the S_{11} envelope. Due to the complexity of the calculation, Fig. 6 is used to give a picture of how the worst in-band S_{11} varies with a changing $\overline{Z_1}$ for different $\overline{Z_2}$. For a fixed $\overline{Z_2}$, the smaller $\overline{Z_1}$ is,

$$\overline{Z_{ISO}} = \frac{2\overline{Z_2}[(j+\omega\overline{C_1})\overline{Z_1}\overline{Z_2}\tan(\theta_1\overline{f_Z})^2 - \overline{Z_1}\tan(\theta_1\overline{f_Z}) - \overline{Z_2}\tan(\theta_2\overline{f_Z})]}{-\overline{Z_1}\overline{Z_2}\tan(\theta_1\overline{f_Z}) + j(\overline{Z_1}\tan(\theta_1\overline{f_Z})^2 + \omega\overline{C_1}\overline{Z_1}\overline{Z_2}\tan(\theta_1\overline{f_Z}) - \overline{Z_2})} \tag{7}$$

$$\overline{C_1}=\frac{1}{8}\cdot\frac{\left(-2\overline{P}\cdot\overline{Z_1}^2+8\overline{Y}\right)\overline{Z_1}\cos(\theta_1\overline{f_m})^2+\left(\left(4+\overline{P}^2\cdot\overline{Z_1}^4+\overline{Z_1}^4-4\overline{P}^2\cdot\overline{Z_1}^2-5\overline{Z_1}^2\right)\sin(\theta_1\overline{f_m})-\overline{P}\cdot\overline{Z_1}\left(\overline{Z_1}^2+4\right)\right)\cos(\theta_1\overline{f_m})+\left(\left(\overline{P}^2+1\right)\overline{Z_1}^4-4\right)\sin(\theta_1\overline{f_m})+\overline{P}\cdot\overline{Z_1}^3-4\overline{P}\cdot\overline{Z_1}}{\pi\overline{f_m}\overline{Z_1}\left(\left(\left(\overline{P}^2+\frac{5}{4}\right)\overline{Z_1}^2-2\right)\cos(\theta_1\overline{f_m})^2+\left(4-\frac{1}{4}\overline{P}\cdot\overline{Z_1}\left(Z_1^2-12\right)\sin(\theta_1\overline{f_m})\right)\cos(\theta_1\overline{f_m})-\frac{1}{4}P\cdot\overline{Z_1}\left(\overline{Z_1}^2+12\right)\sin(\theta_1\overline{f_m})-2-\left(\overline{P}^2+\frac{5}{4}\right)\overline{Z_1}^2\right)} \tag{9}$$

the higher in-band S_{11} would be, because a smaller $\overline{Z_1}$ results in a wider frequency difference between the two reflection zeros. It can also be observed that a smaller $\overline{Z_2}$ results in a wider frequency difference with a fixed $\overline{Z_1}$. Fig. 7 shows an example when $\overline{Z_1}$ equals to 0.4, $\overline{Z_2}$ equals to 2, and θ_1 and θ_2 equal to 30° and 18° at the normalized frequency 1. These two curves imply the frequency tuning range of the power divider and the capacitance range needed of the varactor $\overline{C_1}$ and $\overline{C_2}$. By specifying a specification of $|S_{11}|$, the specified maximum operating frequency $\overline{f_{max}}$ and the minimum operating frequency $\overline{f_{min}}$, the corresponding $\overline{C_{1\min}}$ and $\overline{C_{1\max}}$ can be found using (9) and (11). To simplify the design process, $\overline{C_{1\min}}$ and $\overline{C_{1\max}}$ can be found from Fig. 7 by specifying $\overline{f_{max}}$ and $\overline{f_{min}}$, then $|S_{11}|$ will be evaluated to check if it is better than the specified value at $\overline{f_{max}}$ and $\overline{f_{min}}$. The frequency tuning range also depends on the capacitance tuning range of the varactors. Although a wide frequency tunable range can be achieved theoretically, the range will be limited by the capacitance range of the varactors in practice.

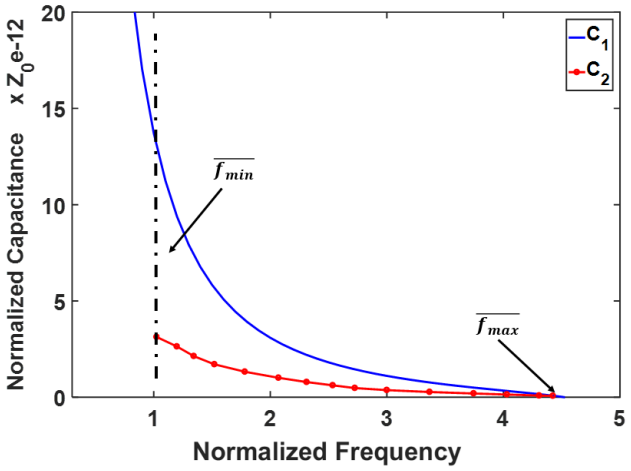

FIGURE 7. Theoretically required capacitance $\overline{C_1}$ and $\overline{C_2}$ versus corresponding frequency with $\overline{Z_2}$=2 when $\overline{Z_1}$=0.4, $\theta_1 = 30°$ and $\theta_2 = 18°$.

E. DESIGN PROCEDURE

The design procedure of the proposed tunable power divider can be summarized as follows.

1) Specify the desired frequency range $\overline{f_{min}}$ and $\overline{f_{max}}$.
2) Choose appropriate θ_1 and θ_2 based on the desired frequency range. Determine $\overline{Z_1}$ and $\overline{Z_2}$ referring to (5) and Fig. 3, making sure the chosen frequency range is slightly wider than the two reflection-zero frequencies. Besides, ensure that the worst in-band S_{11} would meet the specification.
3) Verify if $|S_{11}|$ at $\overline{f_{max}}$ and $\overline{f_{min}}$ would satisfy the specification based on (9) and (11). If not, choose other values for θ_1 and θ_2 and repeat design procedure from 2).
4) Calculate the required capacitance range for varactor $\overline{C_1}$.
5) The resistance $\overline{R}$ and capacitance $\overline{C_2}$ on the isolation circuit can be calculated by substituting all previous design parameters into (7) and (8). The required tuning range of $\overline{C_2}$ on the isolation circuit can be estimated if $\overline{C_1}$ and the corresponding $\overline{f}$ are specified.
6) Choose varactors that can achieve the required tuning ranges of $\overline{C_1}$ and $\overline{C_2}$.
7) After obtaining these parameters, implement the power divider with distributed elements and optimize the physical dimensions with the aid of EM simulation tools. Bias circuits will also be added to tune the varactors in the measurement.

III. DESIGN AND REALIZATION OF THE PROPOSED POWER DIVIDER

One prototype tunable power divider with a frequency tuning range from 1 GHz to 4.2 GHz was designed and fabricated for the validation of the proposed method. Based on the desired tuning range, the electrical lengths of the front and the isolation transmission lines are chosen to be $\theta_1 = 36°$ and $\theta_2 = 18°$ at the normalized frequency 1. According to (5), $\overline{Z_1} = 0.4$ and $\overline{Z_1} = 2.4$ are selected in the design. Hence the characteristic impedances are $Z_1 = 20.3\ \Omega$ and $Z_2 = 120\Omega$. The corresponding $|S_{11}|$ at 1 GHz and 4.2 GHz are both lower than -20 dB. Then the required capacitance range for C_1 is obtained to be 0-7.9 pF. Theoretically, as shown in Fig. 4(d), the achievable frequency tuning range is 4.7:1. For the design parameters in isolation circuit, the resistor R is chosen as 100 Ω according to (7) and (8), and the tuning range of C_2 is 0.2 pF to 2 pF. Based on the desired capacitance tuning ranges of C_1 and C_2, surface mount tuning varactors MA46H202 (7-0.5 pF) are chosen for C_1, while C_2 is realized by an SMV2202 (2.1-0.23 pF). The circuit is designed and fabricated on an RT5880 substrate with a thickness of 0.79 mm and a relative permittivity of 2.2. Table 1 lists the optimized

TABLE 1. Design parameters of the prototype tunable power divider.

Parameters	Value	Parameters	Value
W_1(mm)	4.3	C_1 (pF)	5.1-0.01
W_2(mm)	2.3	C_2 (pF)	2.1-0.2
W_3(mm)	0.5	R (Ω)	100
L_1(mm)	21	V_1 (V)	1.7-20
L_2(mm)	7	V_2 (V)	0-20
L_3(mm)	12		

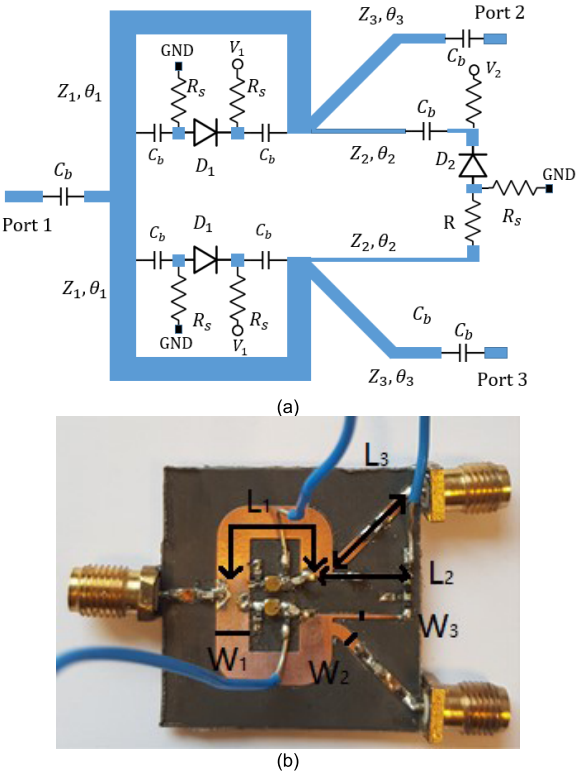

FIGURE 8. (a) The configuration of the proposed power divider and (b) photograph of the fabricated power divider.

parameter values of the prototype tunable power divider. Fig. 8(a) shows the configuration of the design with bias circuits supplying voltages to the varactors. The fabricated circuit is shown in Fig. 8(b). The front transmission lines are bent to connect the varactors in parallel with them. There are three DC bias circuits added to the divider 20 pF capacitors and 10 kΩ resistors are used for DC blocking and RF blocking purposes in the bias circuits, respectively The capacitance C_1 is increased from 0.5 pF to 5.1 pF as the bias voltage for the varactors in the main transmission lines is decreased from 20 V to 0 V. Conversely, the capacitance C_2 is decreased from 2.1 pF to 0.2 pF as the bias voltage on the isolation circuit varies from 0 V to 20 V. Since the capacitance tuning range of the commercially available varactors cannot cover the required tuning range of C_1, the frequency can be only tuned from 0.9 GHz to 2.82 GHz by using these varactors. In order to validate the proposed theory, two capacitors with fixed values of 0.01 pF and 0.2 pF are used in turn here to replace the varactors. Six sampled center frequencies are chosen at 0.9 GHz, 1.7 GHz, 2.1 GHz, 2.8 GHz, 3.45 GHz and 4.2 GHz.

Fig. 9(a)-(d) show the comparison of the simulated and measured S-parameter responses when the divider is tuned to the six sampled frequency bands accordingly. The measured S_{11} and S_{22} are below −20 dB at each band. The insertion loss varies between 3.2 dB and 4 dB, or 0.2 dB to 1 dB above the intrinsic loss of 3 dB. The measured isolation S_{23} is better than −20 dB at most of the sampled frequencies.

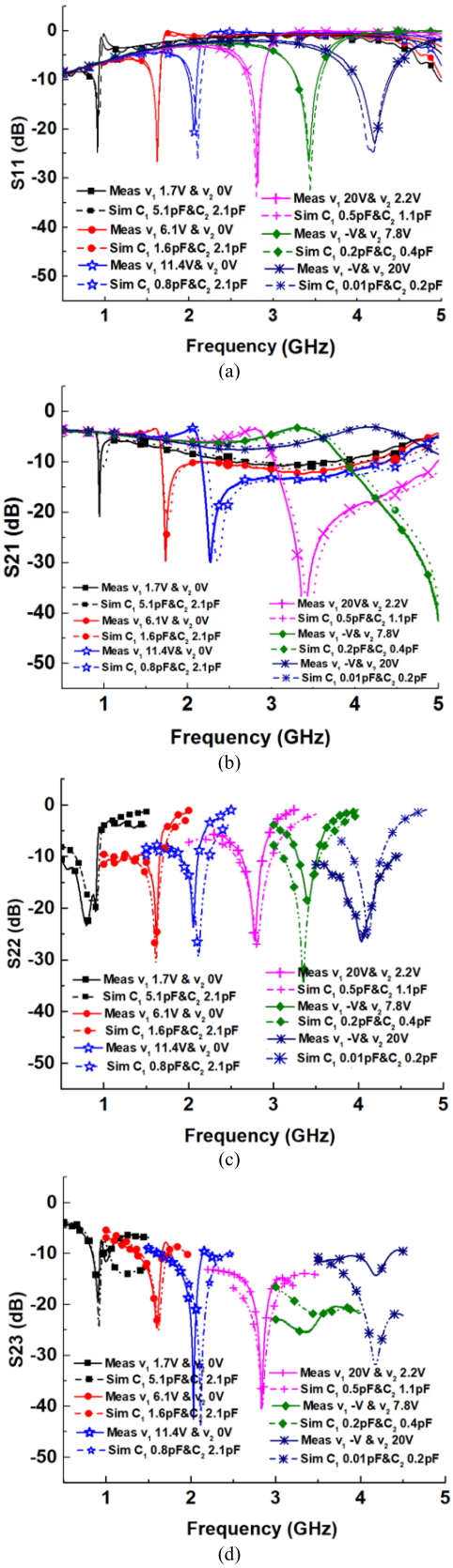

FIGURE 9. Simulated and measured frequency response of the proposed tunable power divider, (a) input reflection $|S_{11}|$, (b) transmission $|S_{21}| = |S_{31}|$, (c) output reflection $|S_{22}| = |S_{33}|$ and (d) isolation $|S_{23}|$.

The isolation is slightly worse at 4.2 GHz with a value of −17 dB, which is probably caused by fabrication errors and the accuracy ofC_2. The achievable tuning range is 3.13:1 by only using the commercial available varactors, while the tuning range can be 4.67:1 with fixed value capacitors as the measured results indicate. Overall, the measured results are in very good agreement with the simulated ones. To show the advantages of the proposed power divider, Table 2 lists the performance comparison between this work and other works reported in recent years. As the table illustrated, the frequency tuning range (when $S_{11} < -20$ dB) for the proposed work is much wider than other relevant works. The measured in-band S_{11} (better than 25 dB) is better than all other works. The circuit is very compact as well for such a wide tuning range.

TABLE 2. Comparison of state-of-the-art reconfigurable power dividers.

Ref.	Tuning Range (GHz)	Return Loss (dB)	Insertion Loss (dB)
[10]	1.3-2.08 (1.6:1)	≥ 20	5.3-2.9
[11]	0.62-0.85 (1.37:1)	≥ 15	5.4-4.8
[13]	0.56-1.39 (2.48:1)	≥ 22	4.5
[14]	0.5-1.3 (2.6:1)	≥ 17	4.6-3.5
[15]	0.83-2.4 (2.89:1)	> 23	3.5-3.3
[16]	0.85-2.4 (2.8:1)	> 20	5.6-2.16
This work	**0.9-4.2 (4.67:1)**$^{+}$	**≥ 25**	**4-3.2**
	0.9-2.82 (3.13:1)*		

$^{+}$: using fixed value capacitors, *: using commercial available varactors

IV. CONCLUSIONS

A compact power divider with a wide frequency tuning range has been proposed and designed in this paper. A pair of varactors are added in parallel with the main transmission lines which introduces a controllable reflection minimum sensitive to the capacitance change. The controllable reflection minimum that moving along with a predictable locus can be determined by the impedance ratio of the main and extra transmission lines. The design equations have been derived and design guidance is provided for determining the design parameters of the power divider. To validate the proposed theory, a prototype with a frequency tuning range from 0.9 GHz to 4.2 GHz has been fabricated and measured. In the measurements, two sets of bias circuits are added to the design for altering the capacitance of the varactors. The center frequency tuning range is dramatically broadened by using this method. The tuning range is 3.13:1 by using commercially available varactors. The range can be extended to 4.67:1 by using fixed value capacitors. To the best of authors' knowledge, the tuning range is superior to all other works. The circuit has a very compact size of $0.2\,\lambda g \times 0.16\,\lambda g$ at the center frequency 2.5 GHz. The measured and simulated results have very good agreement with each other.

APPENDIX

This section discusses the relationship between the value of the added capacitors and the corresponding center frequency. The design in [17] has a reflection minimum at around the original frequency and an additional reflection zero introduced by the added capacitors. There will be two reflection minima in the passband. The frequency tuning range is controlled by changing the value of the added capacitors. The difference of the proposed work is that, by properly choosing $\overline{Z_1 Z_2}$ θ_1 and θ_2, this design only retains the reflection minimum introduced by the added capacitors. As a result, instead of having a tunable bandwidth as in [17], this design will have a tunable center frequency by changing the capacitance.

As the S_{11} curves in Fig. 4 show, the reflection minimum frequency $\overline{f_m}$ is a function of the capacitance $\overline{C_1}$. By choosing a suitable $\overline{C_1}$, a minimum $|S_{11}|$ can be generated at the chosen frequency. In this case, to find the corresponding capacitance $\overline{C_1}$ and the reflection minimum frequency $\overline{f_m}$, take the derivative of $|S_{11}|$ in (3). The derivative should be zero at $\overline{f_m}$:

$$\frac{d\,|S_{11}|}{d\overline{C_1}} = 0 \tag{10}$$

then the expression of $\overline{C_1}$ and $\overline{f_m}$ can be obtained as (9). Eq (9) indicates the correlation of the capacitance range and the frequency tuning range as shown by the blue curve in Fig. 7. To further reveal the relationship between $|S_{11}|$ and the reflection minimum frequency $\overline{f_m}$, the envelope of $|S_{11}|$ needs to be derived. As $\overline{C_1}$ is a function of $\overline{f_m}$ as indicated in (9) by substituting (9) to (1) and (3) the envelope of $|S_{11}|$ can be expressed by:

$$|S_{11}|_{envelope} = \frac{2c\cdot(\overline{YZ_1}^2\sin(\theta_1\overline{f_m})+\overline{Z_1}(1-\cos(\theta_1\overline{f_m})))-d\cdot\overline{Z_1}^2\sin(\theta_1\overline{f_m})}{-2a\cdot(\overline{YZ_1}^2\sin(\theta_1\overline{f_m})+\overline{Z_1}(1-\cos(\theta_1\overline{f_m})))+3b\cdot\overline{Z_1}^2\sin(\theta_1\overline{f_m})} \tag{11}$$

where a, b, c, d, and $\overline{Y}$ can be found in (1) and (3).

REFERENCES

[1] X. Wang, J. Wang, G. Zhang, J.-S. Hong, and W. Wu, "Dual-wideband filtering power divider with good isolation and high selectivity," *IEEE Microw. Wireless Compon. Lett.*, vol. 27, no. 12, pp. 1071–1073, Dec. 2017.

[2] D. Psychogiou, R. Gómez-García, A. C. Guyette, and D. Peroulis, "Reconfigurable single/multi-band filtering power divider based on quasi-bandpass sections," *IEEE Microw. Wireless Compon. Lett.*, vol. 26, no. 3, pp. 684–686, Sep. 2016.

[3] Y. Wu, Y. Liu, Q. Xue, S. Li, and C. Yu, "Analytical design method of multiway dual-band planar power dividers with arbitrary power division," *IEEE Trans. Microw. Theory Techn.*, vol. 58, no. 12, pp. 3832–3841, Dec. 2010.

[4] Y. F. Pan, S. Y. Zheng, Y. M. Pan, Y. X. Li, and Y. L. Long, "A frequency tunable quadrature coupler with wide tuning range of center frequency and wide operating bandwidth," *IEEE Trans. Circuits Syst. II, Exp. Briefs*, vol. 65, no. 7, pp. 864–868, Jul. 2018.

[5] T. Yang and G. M. Rebeiz, "Bandpass-to-bandstop reconfigurable tunable filters with frequency and bandwidth controls," *IEEE Trans. Microw. Theory Techn.*, vol. 65, no. 7, pp. 2288–2297, Jul. 2017.

[6] Z. Wang, J. R. Kelly, P. S. Hall, A. L. Borja, and P. Gardner, "Reconfigurable parallel coupled band notch resonator with wide tuning range," *IEEE Trans. Ind. Electron.*, vol. 61, no. 11, pp. 6316–6326, Nov. 2014.

[7] Z.-H. Chen and Q.-X. Chu, "Dual-band reconfigurable bandpass filter with independently controlled passbands and constant absolute bandwidths," *IEEE Microw. Wireless Compon. Lett.*, vol. 26, no. 2, pp. 92–94, Feb. 2016.

[8] L. Athukorala and D. Budimir, "Open-loop tunable resonators and filters with constant bandwidth," *IET Microw., Antennas Propag.*, vol. 6, no. 7, pp. 800–806, May 2012.

[9] H. Zhu and A. M. Abbosh, "Tunable balanced bandpass filter with wide tuning range of center frequency and bandwidth using compact coupled-line resonator," *IEEE Microw. Wireless Compon. Lett.*, vol. 26, no. 1, pp. 7–9, Jan. 2016.
[10] P.-L. Chi and T. Yang, "A 1.3–2.08 GHz filtering power divider with bandwidth control and high in-band isolation," *IEEE Microw. Wireless Compon. Lett.*, vol. 26, no. 6, pp. 407–409, Jun. 2016.
[11] L. Gao, X. Y. Zhang, and Q. Xue, "Compact tunable filtering power divider with constant absolute bandwidth," *IEEE Trans. Microw. Theory Techn.*, vol. 63, no. 10, pp. 3505–3513, Oct. 2015.
[12] A.-L. Perrier, O. Exshaw, J.-M. Duchamp, and P. Ferrari, "A semi-lumped miniaturized spurious less frequency tunable three-port dividercombiner with 20 dB isolation between output ports," in *IEEE MTT-S Int. Microw. Symp. Dig.*, San Francisco, CA, USA, Jun. 2006, pp. 1714–1717.
[13] X. Shen, Y. Wu, S. Zhou, and Y. Liu, "A novel coupled-line tunable wilkinson power divider with perfect port match and isolation in wide frequency tuning range," *IEEE Trans. Compon., Packag., Manuf. Technol.*, vol. 6, no. 6, pp. 917–925, Jun. 2016.
[14] S.-C. Lin, Y.-M. Chen, P.-Y. Chiou, and S.-F. Chang, "Tunable Wilkinson power divider utilizing parallel-coupled-line-based phase shifters," *IEEE Microw. Wireless Compon. Lett.*, vol. 27, no. 4, pp. 335–337, Apr. 2017.
[15] T. Zhang and W. Che, "A compact tunable power divider with wide tuning frequency range and good reconfigurable responses," *IEEE Trans. Circuits Syst. II, Exp. Briefs*, vol. 63, no. 11, pp. 1054–1058, Nov. 2016.
[16] T. Zhang, X. Wang, and W. Che, "A varactor based frequency-tunable power divider with unequal power dividing ratio," *IEEE Microw. Wireless Compon. Lett.*, vol. 26, no. 8, pp. 589–591, Aug. 2016.
[17] A. Chen, Y. Zhuang, J. Zhou, Y. Huang, and L. Xing, "Design of a broadband wilkinson power divider with wide range tunable bandwidths by adding a pair of capacitors," *IEEE Trans. Circuits Syst. II, Exp. Briefs*, to be published.
[18] S. Horst, R. Bairavasubramanian, M. M. Tentzeris, and J. Papapolymerou, "Modified wilkinson power dividers for millimeter-wave integrated circuits," *IEEE Trans. Microw. Theory Techn.*, vol. 55, no. 11, pp. 2439–2446, Nov. 2007.
[19] X. Wang, I. Sakagami, N. Ito, and A. Mase, "Miniaturised Horst-type Wilkinson power divider with simple layout," *Electron. Lett.*, vol. 49, no. 6, pp. 384–395, 2013.

ANQI CHEN was born in Jingdezhen, China. She received the joint B.Eng. degree in telecommunication engineering from Xi'an Jiaotong-Liverpool University, Suzhou, China, and in electrical and electronics engineering from the University of Liverpool, Liverpool, U.K., in 2014.

She is currently pursuing the Ph.D. degree in electrical and electronics engineering with the University of Liverpool, Liverpool, U.K. Her main research interests include broadband power divider designs and millimeter-wave filter/diplexer designs.

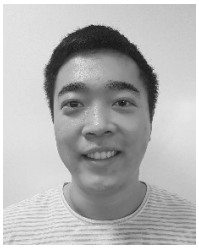

YUAN ZHUANG was born in Baoding, Hebei, China, in 1991. He received the joint B.Eng. degree (Hons.) in telecommunication engineering from Xi'an Jiaotong-Liverpool University, Suzhou, China, and the University of Liverpool, Liverpool, U.K., in 2014. He is currently pursuing the Ph.D. degree with the Department of Electrical Engineering and Electronics, University of Liverpool. His research interests include microwave power amplifiers, filters, electromagnetic energy harvesting, and wireless energy transfer.

YI HUANG (S'91–M'96–SM'06) received the B.Sc. degree in physics from Wuhan University, China, in 1984, the M.Sc. (Eng.) degree in microwave engineering from NRIET, Nanjing, China, in 1987, and the D.Phil. degree in communications from the University of Oxford, U.K., in 1994.

He has been conducting research in the areas of wireless communications, applied electromagnetics, radar, and antennas, since 1987. He spent three years with NRIET as a Radar Engineer and various periods with the Universities of Birmingham, Oxford, and Essex, U.K., as a Member of Research Staff. He was a Research Fellow with British Telecom Labs, in 1994, and then, he joined the Department of Electrical Engineering and Electronics, University of Liverpool, U.K., as a Faculty Member, in 1995, where he is currently a Full Professor in wireless engineering, the Head of the High Frequency Engineering Group, and the Deputy Head of the Department.

He has published over 350 refereed papers in leading international journals and conference proceedings and has authored *Antennas: from Theory to Practice* (John Wiley, 2008) and *Reverberation Chambers: Theory and Applications to EMC and Antenna Measurements* (John Wiley, 2016). He is a Fellow of IET and a Senior Fellow of HEA. He has received many research grants from the research councils, government agencies, charity, EU, and industry, has acted as a consultant to various companies, and has served on a number of national and international technical committees. He has been a Keynote/Invited Speaker and an Organizer of many conferences and workshops, such as WiCom 2006 and 2010, IEEE iWAT2010, LAPC2012, and EuCAP2018. He has been an editor, an associate editor, or a guest editor of five international journals. He is currently the Editor-in-Chief of *Wireless Engineering and Technology*, an Associate Editor of the IEEE Antennas and Wireless Propagation Letters, U.K., and an Ireland Representative of the European Association of Antenna and Propagation.

JIAFENG ZHOU received the B.Sc. degree in radio physics from Nanjing University, Nanjing, China, in 1997, and the Ph.D. degree from the University of Birmingham, Birmingham, U.K., in 2004. His doctoral research concerned high-temperature superconductor microwave filters.

In 1997, for two and a half years, he was with the National Meteorological Satellite Centre of China, Beijing, China. From 2004 to 2006, he was with the University of Birmingham, where his research concerned phased arrays for reflector observing systems. Then, he moved to the Department of Electronic and Electrical Engineering, University of Bristol, Bristol, U.K., until 2013. His research in Bristol was on the development of highly efficient and linear amplifiers. He is currently with the Department of Electrical Engineering and Electronics, University of Liverpool, Liverpool, UK. His past and current research interests include microwave power amplifiers, filters, electromagnetic compatibility, energy harvesting, and wireless power transfer.